

Pressure Effects on the $4f$ Electronic Structure of Light Lanthanides

W.-T. Chiu,¹ D. R. Mortensen,² M. J. Lipp,³ G. Resta,¹ C. J. Jia,⁴ B. Moritz,⁴ T. P. Devereaux,^{4,5,6}
S. Y. Savrasov,¹ G. T. Seidler,² and R. T. Scalettar¹

¹Physics Department, University of California, Davis, California 95616, USA

²Department of Physics, University of Washington, Seattle, Washington 98195-1560, USA

³Physics Division, Lawrence Livermore National Laboratory, Livermore, California 94550, USA

⁴Stanford Institute for Materials and Energy Sciences, SLAC National Accelerator Laboratory,
Menlo Park, California 94025, USA

⁵Geballe Laboratory for Advanced Materials, Stanford University, Stanford, California 94305, USA

⁶Department of Materials Science and Engineering, Stanford University, Stanford, California 94305, USA



(Received 1 December 2018; published 13 February 2019)

Using the satellite structure of the $L\gamma_1$ line in nonresonant x-ray emission spectra, we probe the high-pressure evolution of the bare $4f$ signature of the early light lanthanides at ambient temperature. For Ce and Pr the satellite peak experiences a sudden reduction concurrent with their respective volume collapse (VC) transitions. These new experimental results are supported by calculations using state-of-the-art extended atomic structure codes for Ce and Pr, and also for Nd, which does not exhibit a VC. Our work suggests that changes to the $4f$ occupation are more consistently associated with evolution of the satellite than is the reduction of the $4f$ moment. Indeed, we show that in the case of Ce, mixing of a higher atomic angular momentum state, driven by the increased hybridization, acts to obscure the expected satellite reduction. These measurements emphasize the importance of a unified study of a full set of microscopic observables to obtain the most discerning test of the underlying, fundamental f -electron phenomena at high pressures.

DOI: [10.1103/PhysRevLett.122.066401](https://doi.org/10.1103/PhysRevLett.122.066401)

Introduction.—The physics and chemistry of lanthanides is of critical importance to fields from catalysis [1–3], separations chemistry of nuclear waste [4], to cuprate superconductivity [5,6] and bioscience [7,8]. Despite a rich history, theoretical treatment of these materials remains a fundamental challenge. The difficulty stems primarily from the underlying nature of f -electron states. In materials with partially filled f shells, the electrons occupy narrow strongly correlated energy bands. The resulting electronic interactions exist between the well-understood atomic and uncorrelated band limits and are responsible for a veritable zoo of exotic behaviors: metal-to-insulator transitions [9], superconductivity [10], hidden orderings [11], etc.

A primary example of the challenges in modeling emergent f -electron phenomena is the volume collapse (VC): at high pressures several lanthanides undergo a first-order phase transition that results in large changes to lattice constants and resistivity [12,13]. After the discovery of this phenomenon in Ce [14–16], attention focused on differentiating the Hubbard-Mott (HM) [17,18] picture, which considers the increasing interatomic overlap of $4f$ orbitals with pressure, and the Kondo volume collapse (KVC) [19–24] scenario, where the screening of the $4f$ electrons by broad conduction bands is paramount.

While both HM and KVC theories have had notable successes for Ce, predicting macroscopic observables such as the Ce equation of state [25,26], they are distinguished by

contrasting expectations for the behavior of a foundational microscopic observable: the presence of a $4f$ localized electron and related properties such as the magnetic moment. Upon crossing the VC transition, the complete $4f$ itinerancy predicted by the HM model necessarily extinguishes the $4f$ moment, whereas the hybridization, leading to increased f screening, of the KVC anticipates smaller effects. A significant step forward was the recognition of similarities, e.g. in the evolution with pressure of the density of states, between the two viewpoints [23,27].

Motivated by these observations, Lipp *et al.* presented a study of the pressure evolution of the $L\gamma_1(4d_{3/2} \rightarrow 2p_{1/2})$ nonresonant x-ray emission spectra (NXES) for metallic Ce across its VC [28]. Analogous to the $K\beta'$ feature in $3d$ -transition metal NXES, the $L\gamma_1$ line exhibits a lower-energy satellite feature, $L\gamma'_1$, arising from $(4f, 4d)$ exchange. As a result, the emission intensity is highly sensitive to the presence of a $4f$ electron, raising several fundamental unresolved questions concerning the relative importance of the f occupancy and the moment in the evolution of the $L\gamma'_1$ satellite.

Here we report an extension of the work of Lipp *et al.* to La, Pr, and Nd trivalent metals which lends further insight into the simultaneous occupation, moment, satellite evolution with hybridization. Specifically, we compare the volume-collapsed NXES data to predictions made by advanced atomic calculations, employing density

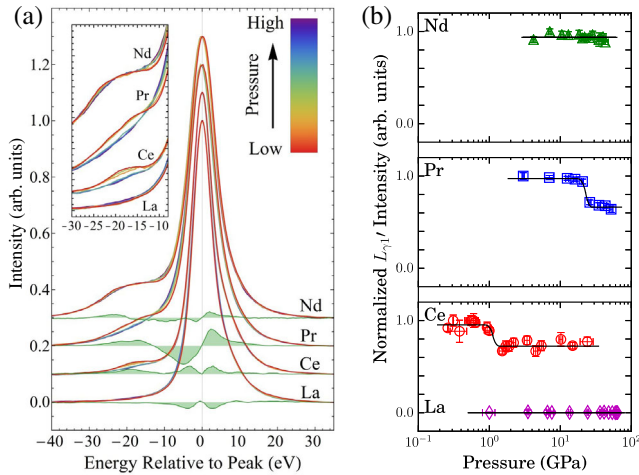


FIG. 1. (a) Experimental $L\gamma_1$ spectra normalized to peak intensity. A nonbroadening, third-order Savitzky-Golay smoothing filter of 5-eV window is applied to each spectrum. For clarity, each element has been offset by 0.1. Also shown is the highest pressure data subtracted from the lowest pressure data for each element (shaded green). (b) Experimental intensity of the $L\gamma_1'$ satellite calculated relative to the main $L\gamma_1$ peak. For Ce, Pr, and Nd the intensities have been normalized to the largest value below the transition for each sample in order to reduce the effects of run-to-run variations. La, which has negligible $L\gamma_1'$ intensity, is left unnormalized. The solid black lines are guides for the eye.

functional theory (DFT)-determined values for the hybridization. The chief conclusion of this Letter is that it is the $4f$ occupation, rather than the moment, which more consistently tracks the intensity of the $L\gamma_1'$ satellite. This opens the door to interpretation of NXES spectroscopy of these materials in which the $4f$ occupation plays a more central role.

Experimental results.—We present the measured $L\gamma_1$ NXES spectra as a function of pressure for La, Ce, Pr, and Nd in Fig. 1. For clarity, the data in Fig. 1(a) have been smoothed using a nonbroadening third-order Savitzky-Golay filter with a 5 eV window (comparable to the lifetime-limited resolution of 3.7–4.0 eV) and normalized to peak intensity. Raw data (without smoothing) is used in Fig. 2 and the analysis below. Also shown is the highest pressure data subtracted from lowest pressure for each element, to highlight the influence of pressure on the spectral shape. In Fig. 1(b) we present a quantitative extraction of the relative $L\gamma_1'$ intensities. While comparison to La is a useful diagnostic for Ce, as shown above, it does not work well for Pr and Nd where the differences in the multiplet structure of the $L\gamma_1$ peak prevent a direct cross evaluation. Instead, we fit the spectrum to a sum of Lorentzians: one to model the contribution from the main peak in the satellite region and the others (two for Pr and three for Nd) to fit the $L\gamma_1'$ peak proper. This procedure has previously been used for Ce NXES [28]. The results shown in Fig. 1(b) reflect the spectral weight of the shoulder

relative to the main peak. For Ce, Pr, and Nd these results have been normalized to the largest intensity below the transition for each sample to eliminate small run-to-run variations due to differences in spectrometer tune-up that would otherwise prevent direct comparison.

La, which was found to have constant, negligible satellite intensity at all pressures, is left unnormalized. Nd is similarly found to have negligible variation even during the minor change in spectral shape upon the fcc to distorted-fcc transition at 18.0 GPa discussed below. Further measurements are required to determine if Nd eventually undergoes $L\gamma_1'$ reduction, similar to Ce and Pr, upon reaching its delocalized $\alpha-U$ phase at ~ 100 GPa [29]. Before interpreting these results, however, some brief context is needed on known behavior of the light lanthanides under pressure and on the underlying physics of the $L\gamma_1$ NXES spectra.

First, under pressure the lanthanide crystal structures initially pass through several high-symmetry transformations of different stacking sequences of close-packed layers, later transitioning to low-symmetry early-actinide-like phases indicative of f -electron bonding [30–32]. While in Pr this transition is accompanied with a large VC ($\sim 10\%$) [33–37], Nd reaches its low-symmetry $\alpha-U$ structure entirely through smooth transformations [29]. Hence, Nd does not exhibit a VC transition. Ce is a unique case as it experiences an isostructural (fcc) VC (15%), unassociated with the high-to-low symmetry transition. For this reason its VC is thought to be primarily electronically driven.

Second, as demonstrated by Lipp *et al.* [28], NXES provides a sensitive measure of the evolution of intrinsic $4f$ signatures in Ce. In $L\gamma_1$ NXES a high-energy photon, tuned well above the $L_2(2p_{1/2})$ edge, promotes a $2p$ electron into the continuum. The resulting core-level vacancy is unstable and may be filled by a $4d_{3/2}$ electron accompanied by either photon emission ($L\gamma_1$ x-ray fluorescence) or Auger electron ejection. When the lanthanide species has a nonzero $4f$ occupancy, a low-energy satellite ($L\gamma_1'$) appears below the main $L\gamma_1$ fluorescence peak due to intra-atomic exchange between $4f$ and $4d$ orbitals [38]. The relative intensity and position of the $L\gamma_1'$ shoulder reflects the strength of the coupling and is directly sensitive to the $4f$ properties [39,40].

These observations give rise to a fundamental question: To what extent is the evolution of the satellite a probe of the bare moment or of the occupation? This question complements the well-considered debate concerning whether the VC itself is associated with destruction of the bare moment or its screening. Of course, the moment is linked to the occupation, so the answer is expected to be intertwined. In the theoretical work to follow we will compute the satellite peak, occupation, and bare moment as functions of hybridization (pressure) to lend insight into these issues.

With these details in mind, we return to Fig. 1. First, note that the La $L\gamma_1$ NXES spectra show no $L\gamma_1'$ exchange peak up to 64.0 ± 3.0 GPa, beyond the reentrant fcc phase

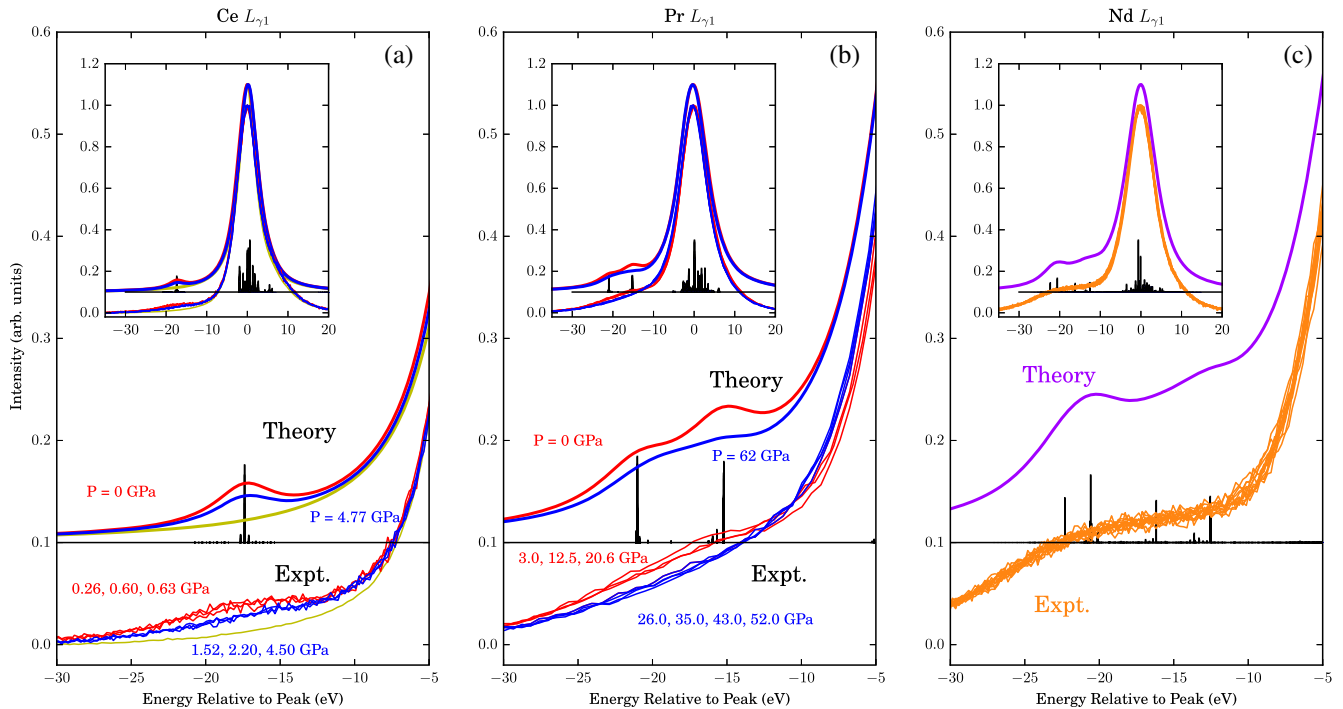


FIG. 2. The shoulder peak (satellite) region of the experimental and calculated x-ray emission spectra for light lanthanide metals. The red (blue) curves in (a) for Ce and (b) for Pr are at low (high) pressure. In the theory spectra, low pressure is modeled using parameters at $P = 0$ GPa, and the blue curves are obtained using high-pressure parameters (4.77 GPa for Ce and 62 GPa for Pr). The yellow curves in (a) are results of lanthanum for a zero shoulder peak reference. (c) The Nd $L\gamma_1$ spectra do not change with pressure up to 43 GPa. Here, experimental and theoretical results are shown as orange and purple, respectively. The calculated spectra are shifted by +0.1. Insets show the full $L\gamma_1$ spectra. The vertical black lines are the calculated transition probabilities before broadening at zero pressure.

starting at 60 GPa [41], indicating no change from its nominally $4f^0$ configuration. This null result indicates that the changes observed in Ce, Pr, and Nd $L\gamma_1'$ peaks are physically meaningful. That being said, La does display an apparent broadening of the main $L\gamma_1$ peak (on the order of ~ 0.5 eV) with increased pressure. We propose that this effect is due to increased splitting in the multiplet structure underlying the $L\gamma_1$ peak. The changing spectral shape therefore likely contains valuable information on the evolving $4d$ -electron interactions [42] and thus merits future theoretical consideration.

Second, in contrast to La ($4f^0$), Ce and Pr, which are nominally $4f^1$ and $4f^2$ at ambient conditions, exhibit large and sudden decreases in $L\gamma_1'$ intensity concurrent with the VC transitions (0.9 and 20.0 GPa, respectively). Taken naively, this result could be used as evidence in support of the HM model as described above. However, it must be noted that although the increased $4f - 5d$ hybridization predicted by KVC invariably mixes the $4f$ electrons out of their native orbitals, leading to deviations from the ground state electronic configuration, the hybridization causes a rise in the $f^{n\pm 1}$ configuration weights at the expense of the sharp, low-pressure f^n configuration. Indeed, this phenomenon has already been experimentally observed in resonant inelastic x-ray scattering measurements for both

Ce and Pr [43,44]. As each configuration carries its own moment, such variations would necessarily modulate the $L\gamma_1'$ feature.

This potentially ambiguous result can be clarified by comparison to La, for which there is a true zero $4f$ occupancy. The f -electron signature, Fig. 2(a), while reduced, does not fully vanish in the collapsed-phase Ce spectrum, inconsistent with a complete Mott delocalization. Pr NXES, which has a broader main $L\gamma_1$ peak than Ce, does not lend itself to a direct La comparison. The persistence of its $4f$ hallmark will be demonstrated below.

Nd, which is not subject to any large VC transition, shows a minor change in the $L\gamma_1'$ peak (Fig. 1). There is a shift in $L\gamma_1'$ to a slightly higher energy (~ 0.3 eV) concomitant with a transition from a fcc to a distorted-fcc structure at ~ 18.0 GPa [29,45]. As the $4f$ electrons are still localized at this pressure, the observed shift is likely due to subtle changes in the relative positioning and subsequent electron transfer between conduction subbands which are known to occur during the high-symmetry transformations [46]. As will be shown shortly, however, the normalized amplitude of the $L\gamma_1'$ peak is unchanged during this shift. We note that this change is not associated with any known delocalization transition; for example, prior diffraction and electrical resistivity measurements suggest that $4f$

delocalization in Nd occurs gradually beginning only at 100 GPa [46].

Theoretical predictions and results.—To this point we have made qualitative arguments regarding the pressure dependence of the $L\gamma'_1$ shoulder. We now supplement this with a theoretical treatment. In the Kramers-Heisenberg formalism, the NXES intensity is [47,48]

$$I_g(\omega) \propto \sum_j \left| \sum_i \frac{\langle j|\hat{T}|i\rangle\langle i|\hat{a}_c|g\rangle}{E_j - E_i - \omega - i\Gamma_i} \right|^2, \quad (1)$$

where \hat{T} is the dipole operator for $4d \rightarrow 2p$ transitions, \hat{a}_c is the annihilation operator of the core electron, ω is the energy of emission, and $|g\rangle$, $|i\rangle$, and $|j\rangle$ are the ground, intermediate, and final states, respectively, with energies E_g , E_i , and E_j . To account for finite temperature, Eq. (1) is modified assuming a Boltzmann distribution:

$$\langle I(\omega) \rangle_T = \sum_g e^{-E_g/kT} I_g(\omega) / \sum_g e^{-E_g/kT}, \quad (2)$$

where T is the working temperature (300 K in the analysis below) and k is the Boltzmann constant.

The electron states are determined by diagonalizing a Hamiltonian combining a single impurity Anderson model [48,49] with interactions accounting for multiplet terms. The pressure-dependent hybridization V is calculated by a first-principles approach [50]. In Fig. 2, we present the results of these calculations compared to the experimental data. It must be noted that in the theoretical results, the atomic multiplet features composing the $L\gamma'_1$ satellite are sharper than they appear in experiment. This is a consequence of using only five discrete conduction orbitals in place of the true, broad $5d$ band for hybridization. Such an approximation is necessary to ensure reasonable computation time. Nevertheless, it is clearly demonstrated that the steplike decrease in $L\gamma'_1$ intensity observed in Ce and Pr concomitant with VC is consistent with a sudden increase of $4f$ -conduction band hybridization as predicted by the KVC model.

The physical observables are calculated by

$$A_T = \frac{\sum_g e^{-E_g/kT} \langle g|\hat{A}|g\rangle}{\sum_g e^{-E_g/kT}}, \quad (3)$$

where $\hat{A} = \hat{n}_f = \sum_{\nu} a_{f,\nu}^\dagger a_{f,\nu}$ for obtaining the $4f$ occupation number and $\hat{A} = \hat{J}^2$ for the local $4f$ moment. The values are normalized to zero pressure, as shown in Fig. 3. The results demonstrate that both $4f$ occupancy and $L\gamma'_1$ intensity decrease as pressure goes up, with the $L\gamma'_1$ intensity doing so at a slightly faster rate. The important point, however, is that a persistent $L\gamma'_1$ feature is indicative of continued $4f$ localization.

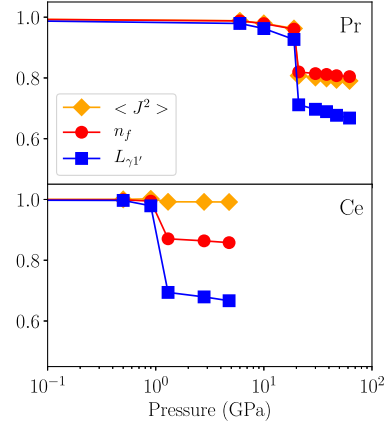


FIG. 3. The calculated bare magnetic moments ($\langle J^2 \rangle$), $4f$ occupation numbers (n_f), and shoulder peak intensities ($L_{\gamma'1}$) at various pressures for cerium and praseodymium. All quantities are normalized to their zero-pressure value.

The local moment $\langle J^2 \rangle$ behavior is more complicated, since it depends on not only the $4f$ occupancy but also the occupancy of each j level. Taking Ce first, there are $j = 5/2$ and $j = 7/2$ states with spin-orbit coupling. The occupancy of the levels will be a function of the $4f$ on-site energy, ϵ_f , and the hybridization V , as shown in Appendix A of Ref. [61]. In the $V = 0$ limit, the system follows Hund's rule and only $j = 5/2$ ($\langle J^2 \rangle = 8.75$) is occupied. As V turns on, the occupancy of $j = 7/2$ will grow, and the ratio ($n_{7/2}/n_f$) depends on ϵ_f : When ϵ_f is deep in the valence band, the ratio is small, so $\langle J^2 \rangle$ decreases as $n_f \sim n_{5/2}$ decreases with rising V ; in the other limit, when $n_{7/2}/n_f$ reaches $8/14$ at large V , $\langle J^2 \rangle$ increases as V goes up [62]. For Ce, $\langle J^2 \rangle$, Fig. 3 (bottom), the effects from decreasing n_f and increasing $n_{7/2}/n_f$ compensate each other. $\langle J^2 \rangle$ stays almost constant as pressure goes up. Reference [28] reached a similar conclusion concerning the more paramount importance of n_f in tracking the satellite peak, ascribing the (somewhat larger) change reported there in $\langle J^2 \rangle$ mostly to the change in occupation, so that the latter is more fundamental. Our conclusions are even somewhat stronger in implicating the occupation, since $\langle J^2 \rangle$ is almost completely stable.

Figure 3 (top) similarly emphasizes that an abrupt change in $4f$ occupation also occurs through the Pr VC transition, concomitant with the satellite peak evolution. $\langle J^2 \rangle$ is also reduced. This is in contrast to results reported for Pr in Ref. [62]. The reason is the challenge of considering the full set of rotationally invariant Coulomb interactions within dynamic mean field theory. Reference [62] included spin-orbit coupling but only the direct Coulomb interaction. As a result, $\langle J^2 \rangle$ for Pr and even Nd behaved similarly to Ce: $\langle J^2 \rangle$ increases when volume decreases, because only a higher $j = 7/2$ level is mixed in the ground state as hybridization turns on. We

include all interactions, so all multiplet states of Pr mix with the Hund's rule ground state when V is nonzero. In the pressure range of our calculation, $\langle J^2 \rangle$ drops but retains $\sim 80\%$ of its ambient value across the VC transition. Reproducing the experimental features, both Ce and Pr $L\gamma'_1$ intensities undergo a large, sudden drop with the VC. These reductions, however, are incomplete with $\sim 70\%$ and $\sim 65\%$ for Ce and Pr, respectively.

Conclusion.—We have presented a high-quality dataset of high-pressure $L\gamma'_1$ NXES useful for the characterization of bare $4f$ electron evolution in the early light lanthanide metals. These data are supported by state-of-the-art modified atomic calculations which extend previous work performed on Ce alone to Pr and Nd. A central conclusion concerns the evolution of the $4f$ occupation. There are increasing indications that the most unified picture of the NXES spectra for the light lanthanides and their compounds might be provided by n_f [63,64] rather than measures of the $4f$ magnetism—the number of Bohr magnetons, total angular momentum. Our calculations provide crucial evidence of a clear relationship between $L\gamma'_1$ intensity and $4f$ -conduction band hybridization. Thus, despite the importance of Kondo screening of the moments in the volume collapse of Ce and Pr, the interpretation of their NXES spectra appears also to fit in a broader, common picture focused on $4f$ occupation.

NXES studies were performed under the auspices of the U.S. Department of Energy by Lawrence Livermore National Laboratory under Contract No. DE-AC52-07NA27344 and at HPCAT (Sector 16), Advanced Photon Source (APS), Argonne National Laboratory. HPCAT operations are supported by DOE-NNSA under Award No. DE-NA0001974 and DOE-BES under Award No. DE-FG02-99ER45775, with partial instrumentation funding by NSF. The Advanced Photon Source is a U.S. Department of Energy (DOE) Office of Science User Facility operated for the DOE Office of Science by Argonne National Laboratory under Contract No. DE-AC02-06CH11357. The theoretical work of W.-T. C. and R. T. S. was supported by the Stewardship Sciences Academic Alliance program under Grant No. DE-NA0002908. Portions of the computational work were performed using the resources of the National Energy Research Scientific Computing Center supported by the U.S. Department of Energy, Office of Science, under Contract No. DE-AC02-05CH11231. C. J. J., B. M., and T. P. D. at SLAC are supported by the U.S. Department of Energy, Office of Basic Energy Sciences, Materials Sciences and Engineering Division, under Contract No. DE-AC02-76SF00515 for the atomic multiplet calculations and interpretation. D. R. M. and G. T. S. acknowledge support from the U.S. Department of Energy, Office of Basic Energy Sciences, under Grant No. DE-SC0002194 and also by the Office of Science, Fusion Energy Sciences, under Grant No. DE-SC0016251. G. R. and S. Y. S. were supported by

the U.S. National Science Foundation Grant No. DMR-1411336 (S. Y. S).

- [1] F. T. Edelmann, *Chem. Soc. Rev.* **41**, 7657 (2012).
- [2] B. T. Kilbourn, *J. Less-Common Met.* **126**, 101 (1986).
- [3] M. Shibusaki and N. Yoshikawa, *Chem. Rev.* **102**, 2187 (2002).
- [4] K. Nash and G. Lumetta, *Advanced Separation Techniques for Nuclear Fuel Reprocessing and Radioactive Waste Treatment* (Woodhead Publishing Limited, Cambridge, England, 2011).
- [5] J. G. Bednorz and K. A. Muller, *Z. Phys. B* **64**, 189 (1986).
- [6] A. L. Ivanovskii, *Phys. Usp.* **51**, 1229 (2008).
- [7] J. P. Chen, S. Patil, S. Seal, and J. F. McGinnis, *Nat. Nanotechnol.* **1**, 142 (2006).
- [8] C. Bouzigues, T. Gacoïn, and A. Alexandrou, *ACS Nano* **5**, 8488 (2011).
- [9] M. Imada, A. Fujimori, and Y. Tokura, *Rev. Mod. Phys.* **70**, 1039 (1998).
- [10] C. Pfleiderer, *Rev. Mod. Phys.* **81**, 1551 (2009).
- [11] P. Chandra, P. Coleman, J. A. Mydosh, and V. Tripathi, *Nature (London)* **417**, 831 (2002).
- [12] V. S. Egorov and I. N. Khlyustikov, in *Handbook of Physical Quantities*, edited by I. S. Grigor'ev and E. Z. Meilikhov (English translation by A. A. Radzig) (CRC, Boca Raton, FL, 1997), pp. 549–572.
- [13] N. Velisavljevic, K. M. MacMinn, Y. K. Vohra, and S. T. Weir, *Appl. Phys. Lett.* **84**, 927 (2004).
- [14] P. W. Bridgman, *Proc. Am. Acad. Arts Sci.* **62**, 207 (1927).
- [15] P. W. Bridgman, *Proc. Am. Acad. Arts Sci.* **76**, 71 (1948).
- [16] A. W. Lawson and T. Y. Tang, *Phys. Rev.* **76**, 301 (1949).
- [17] B. Johansson, *Philos. Mag.* **30**, 469 (1974).
- [18] B. Johansson, *Phys. Rev. B* **11**, 2740 (1975).
- [19] J. W. Allen and R. M. Martin, *Phys. Rev. Lett.* **49**, 1106 (1982).
- [20] M. Lavagna, C. Lacroix, and M. Cyrot, *Phys. Lett.* **90A**, 210 (1982).
- [21] J. W. Allen and L. Z. Liu, *Phys. Rev. B* **46**, 5047 (1992).
- [22] A. K. McMahan, K. Held, and R. T. Scalettar, *Phys. Rev. B* **67**, 075108 (2003).
- [23] K. Held, A. K. McMahan, and R. T. Scalettar, *Phys. Rev. Lett.* **87**, 276404 (2001).
- [24] K. Haule, V. Oudovenko, S. Y. Savrasov, and G. Kotliar, *Phys. Rev. Lett.* **94**, 036401 (2005).
- [25] M. J. Lipp, D. Jackson, H. Cynn, C. Aracne, W. J. Evans, and A. K. McMahan, *Phys. Rev. Lett.* **101**, 165703 (2008).
- [26] B. Johansson, A. V. Ruban, and I. A. Abrikosov, *Phys. Rev. Lett.* **102**, 189601 (2009).
- [27] M. B. Zöfl, I. A. Nekrasov, Th. Pruschke, V. I. Anisimov, and J. Keller, *Phys. Rev. Lett.* **87**, 276403 (2001).
- [28] M. J. Lipp, A. P. Sorini, J. Bradley, B. Maddox, K. T. Moore, H. Cynn, T. P. Devereaux, Y. Xiao, P. Chow, and W. J. Evans, *Phys. Rev. Lett.* **109**, 195705 (2012).
- [29] G. N. Chesnut and Y. K. Vohra, *Phys. Rev. B* **61**, R3768 (2000).
- [30] W. B. Holzapfel, *J. Alloys Compd.* **223**, 170 (1995).
- [31] A. K. McMahan, C. Huscroft, R. T. Scalettar, and E. L. Pollock, *J. Comput. Aided Mater. Des.* **5**, 131 (1998).

- [32] A. Lindbaum, S. Heathman, T. Le Bihan, R. G. Haire, M. Idiri, and G. H. Lander, *J. Phys. Condens. Matter* **15**, S2297 (2003).
- [33] J. S. Olsen, L. Gerward, U. Benedict, and J.-P. Itié, *Physica (Amsterdam)* **133B**, 129 (1985).
- [34] Y. K. Vohra, S. L. Beaver, J. Akella, C. A. Ruddle, and S. T. Weir, *J. Appl. Phys.* **85**, 2451 (1999).
- [35] H. K. Mao, R. M. Hazen, P. M. Bell, and J. Wittig, *J. Appl. Phys.* **52**, 4572 (1981).
- [36] G. S. Smith and J. Akella, *J. Appl. Phys.* **53**, 9212 (1982).
- [37] B. J. Baer, H. Cynn, V. Iota, C. S. Yoo, and G. Y. Shen, *Phys. Rev. B* **67**, 134115 (2003).
- [38] P. Glatzel and U. Bergmann, *Coord. Chem. Rev.* **249**, 65 (2005).
- [39] K. Jouda, S. Tanaka, and O. Aita, *J. Phys. Condens. Matter* **9**, 10789 (1997).
- [40] S. Tanaka, H. Ogasawara, K. Okada, and A. Kotani, *J. Phys. Soc. Jpn.* **64**, 2225 (1995).
- [41] F. Porsch and W. B. Holzapfel, *Phys. Rev. Lett.* **70**, 4087 (1993).
- [42] F. de Groot, *Coord. Chem. Rev.* **249**, 31 (2005).
- [43] J. P. Rueff, J. P. Itié, M. Taguchi, C. F. Hague, J. M. Mariot, R. Delaunay, J. P. Kappler, and N. Jaouen, *Phys. Rev. Lett.* **96**, 237403 (2006).
- [44] J. A. Bradley, K. T. Moore, M. J. Lipp, B. A. Mattern, J. I. Pacold, G. T. Seidler, P. Chow, E. Rod, Y. M. Xiao, and W. J. Evans, *Phys. Rev. B* **85**, 100102(R) (2012).
- [45] J. Akella, S. T. Weir, Y. K. Vohra, H. Prokop, S. A. Catledge, and G. N. Chesnut, *J. Phys. Condens. Matter* **11**, 6515 (1999).
- [46] N. Velisavljevic, Y. K. Vohra, and S. T. Weir, *High Press. Res.* **25**, 137 (2005).
- [47] L. J. P. Ament, M. van Veenendaal, T. P. Devereaux, J. P. Hill, and J. van den Brink, *Rev. Mod. Phys.* **83**, 705 (2011).
- [48] A. Kotani and S. Shin, *Rev. Mod. Phys.* **73**, 203 (2001).
- [49] P. W. Anderson, *Phys. Rev.* **124**, 41 (1961).
- [50] See Supplemental Material at <http://link.aps.org/supplemental/10.1103/PhysRevLett.122.066401> for experimental and theoretical details, which includes Refs. [28, 31, 33, 37, 40, 45, 51–60].
- [51] S. Heald, G. T. Seidler, D. Mortensen, B. Mattern, J. A. Bradley, N. Hess, and M. Bowden, *Proc. SPIE Int. Soc. Opt. Eng.* **8502**, 85020I (2012).
- [52] D. R. Mortensen, G. T. Seidler, J. A. Bradley, M. J. Lipp, W. J. Evans, P. Chow, Y. M. Xiao, G. Boman, and M. E. Bowden, *Rev. Sci. Instrum.* **84**, 083908 (2013).
- [53] M. T. Czyżyk and G. A. Sawatzky, *Phys. Rev. B* **49**, 14211 (1994).
- [54] R. D. Cowan, *The Theory of Atomic Structure and Spectra* (University of California Press, Berkeley, CA, 1981).
- [55] O. Gunnarsson, O. K. Andersen, O. Jepsen, and J. Zaanen, *Phys. Rev. B* **39**, 1708 (1989).
- [56] M. J. Han, X. Wan, and S. Y. Savrasov, *Phys. Rev. B* **78**, 060401(R) (2008).
- [57] J. H. Shim, K. Haule, S. Savrasov, and G. Kotliar, *Phys. Rev. Lett.* **101**, 126403 (2008).
- [58] A. Toropova, C. A. Marianetti, K. Haule, and G. Kotliar, *Phys. Rev. B* **76**, 155126 (2007).
- [59] K. Haule, C.-H. Yee, and K. Kim, *Phys. Rev. B* **81**, 195107 (2010).
- [60] J. R. Schrieffer and P. A. Wolff, *Phys. Rev.* **149**, 491 (1966).
- [61] O. Gunnarsson and K. Schönhammer *Phys. Rev. B* **28**, 4315 (1983).
- [62] A. K. McMahan, *Phys. Rev. B* **72**, 115125 (2005).
- [63] M. J. Lipp, J. R. Jeffries, H. Cynn, J.-H. Park Klepeis, W. J. Evans, D. R. Mortensen, G. T. Seidler, Y. Xiao, and P. Chow, *Phys. Rev. B* **93**, 064106 (2016).
- [64] A. Bianconi, A. Kotani, K. Okada, R. Giorgi, A. Gargano, A. Marcelli, and T. Miyahara, *Phys. Rev. B* **38**, 3433 (1988).